Electronic states of perovskite-type $Ce_{1-x}Sr_xTiO_3$ and $CeTiO_{3+y/2}$ systems with a metal - insulator transition

1997 J. Phys.: Condens. Matter 9 5623

(http://iopscience.iop.org/0953-8984/9/26/010)

J. Phys.: Condens. Matter **9** (1997) 5623–5634. Printed in the UK PII: S0953-8984(97)81817-6

Electronic states of perovskite-type $Ce_{1-x}Sr_xTiO_3$ and $CeTiO_{3+y/2}$ systems with a metal–insulator transition

Masashige Onoda and Masaaki Yasumoto

Institute of Physics, University of Tsukuba, Tennodai, Tsukuba 305, Japan

Received 13 February 1997

Abstract. Electronic states of the perovskite systems $Ce_{1-x}Sr_xTiO_3$ ($0 \leqslant x \leqslant 1$) and $CeTiO_{3+y/2}$ ($-0.36 \leqslant y \leqslant 0.44$) with a metal–insulator crossover have been studied through measurements of x-ray diffraction, electrical resistivity, thermoelectric power, Hall coefficient and magnetization. The $Ce_{1-x}Sr_xTiO_3$ system that is pseudotetragonal for $x \leqslant 0.4$ and cubic for $x \geqslant 0.5$ is characterized as follows: (i) $0 \leqslant x < 0.02$, variable-range hopping-like insulators; (ii) $0.04 \leqslant x \leqslant 0.4$, highly correlated metals accompanied by a significant Jahn–Teller effect, a band dispersion anomaly and cant magnetism for $x \leqslant 0.1$; (iii) $0.5 \leqslant x \leqslant 0.9$, metals with a mean free path comparable with the Ti–Ti distance; (iv) $x = 1$, band insulators. The properties of $CeTiO_{3+y/2}$ against y are rather similar to those of $Ce_{1-x}Sr_xTiO_3$ against x, but larger random potentials due to the atomic deficiency in the former system give rise to strong electron localization. For the metallic state near the crossover between the Mott–Hubbard insulator and metal, both an enhancement of the conduction electron mass and the antiferromagnetic correlation effect should be considered.

1. Introduction

Various 3d transition-metal ternary oxides with unfilled d orbitals have been studied in order to clarify peculiar properties in correlated-electron or electron–phonon-coupling systems. Perovskite-type oxides with the chemical formula $MTiO_3$ or MVO_3, where M is an alkaline-earth or rare-earth element, have been investigated intensively, since the electron concentration or band width can be controlled easily through the substitution of M ions. For example, $La_{1-x}Sr_xTiO_3$ and $La_{1-x}Sr_xVO_3$ with $0 \leqslant x \leqslant 1$ may be such systems and exhibit a metal–insulator transition at certain x [1–13]. Here, $SrTiO_3$ (d^0 configuration) and $SrVO_3$ (d^1 configuration) with $x = 1$ are a band insulator and a Fermi-liquid compound, respectively. On the other hand, $LaTiO_3$ (d^1) and $LaVO_3$ (d^2) with $x = 0$ are both Mott–Hubbard insulator like. The structures at room temperature are of $GdFeO_3$ type with $a \simeq b \simeq \sqrt{2}a_c$ and $c \simeq 2a_c$, where a_c is the simple-cubic perovskite dimension as applied to $SrTiO_3$ or $SrVO_3$.

The Pauli paramagnetic susceptibility and electronic specific heat measurements of the $La_{1-x}Sr_xTiO_3$ system have indicated that the conduction electron mass in the metallic phase increases drastically as the system approaches the metal–insulator boundary with decreasing x [2, 7]. Recently, the electronic states of $RTiO_3$ (R = La, Ce, Pr or Nd) located near the boundary between the Mott–Hubbard insulator and the correlated metal have been investigated [13]. The transport properties depend on an inhomogeneity of the atomic concentration and/or comparability of the correlation energy U and the band width W characterized by a change in the transfer integral of the Ti–O–Ti pathway due to TiO_6 tilting.

0953-8984/97/265623+12$19.50

The dominant contribution to transport of the oxygen-deficient La and nearly stoichiometric Ce compounds may be by hopping at high temperatures and by extended states at low temperatures. The compounds with excess oxygen (or cation deficiencies) are highly or weakly correlated metals which depend on the magnitudes of their band widths as well as random potentials. Based on the temperature dependence of magnetic susceptibility of various La compounds, the existence of the pseudogap in the density of states for the highly correlated metals has been postulated.

This paper reports a study on the electronic states of the $Ce_{1-x}Sr_xTiO_3$ and $CeTiO_{3+y/2}$ systems. These systems remove x and y electrons from one electron per Ti site by changing x and y for positive y. Here, positive y means that the actual cation concentration is $(1 + y/6)^{-1}$ for the stoichiometric oxygen concentration. For the negative case, y electrons are added. Thus, one can study electronic states in a wide range of electron concentrations. We have measured x-ray diffraction, electrical resistivity, thermoelectric power, Hall coefficient and magnetization in order to discuss the properties of 3d electrons with d^2, d^1 and d^0 configurations from various viewpoints. The experimental methods are provided in section 2. Section 3 describes the experimental results and basic items with respect to the crystal symmetry and electronic states. In section 4, the electronic states are discussed synthetically based on various experimental results. Section 5 is devoted to a conclusion.

2. Experiments

Polycrystalline specimens of the $Ce_{1-x}Sr_xTiO_3$ and $CeTiO_{3+y/2}$ systems were prepared from a congruent melt with an Ar arc furnace. Here, starting materials were CeO_2 (99.9% purity), SrO (99% purity), TiO_2 (99.9% purity) and Ti metal (99.9% purity). Thermogravimetric analysis (TGA) and electron-probe microanalysis (EPMA) were done to estimate the oxygen concentration of $CeTiO_{3+y/2}$ and the cation concentration ratio of both the systems, respectively.

X-ray powder diffraction patterns were obtained with Cu Kα radiation at 290 K using a two-circle diffractometer. The electrical resistivity was measured with a DC four-terminal method between 4.2 and 300 K. The thermoelectric power was measured by a DC method between 4.2 and 350 K. The Hall coefficient was determined at 290 K using a field of up to 15 kOe. The magnetization was obtained by the Faraday method from 4.2 to 800 K, where a field of up to about 8 kOe was applied. The magnetic susceptibility was estimated from the linear coefficient of magnetization versus field (M–H) curve with a decreasing field.

3. Results and analyses

3.1. Lattice constant, oxygen concentration and cation ratio

The oxygen concentration in $CeTiO_{3+y/2}$ is that estimated by TGA with an accuracy to 0.01. The cation concentration ratio estimated by EPMA nearly agrees with the nominal value. We shall use the nominal composition as that of the compound.

The lattice constants as a function of x and y are shown in figure 1. Here, the crystal symmetry of $Ce_{1-x}Sr_xTiO_3$ with $x \geqslant 0.5$ is nearly cubic, while those of other compounds are tetragonal or pseudotetragonal. For convenience, the cubic lattice constant a_c is transformed into the tetragonal constant by the relations $a_t = \sqrt{2}a_c$ and $c_t = 2a_c$. The plot for $Ce_{1-x}Sr_xTiO_3$ is compatible with that for $CeTiO_{3+y/2}$, suggesting that the lattice constants are scaled by the nominal Ti valence, $3 + x$ or $3 + y$. A change in the lattice

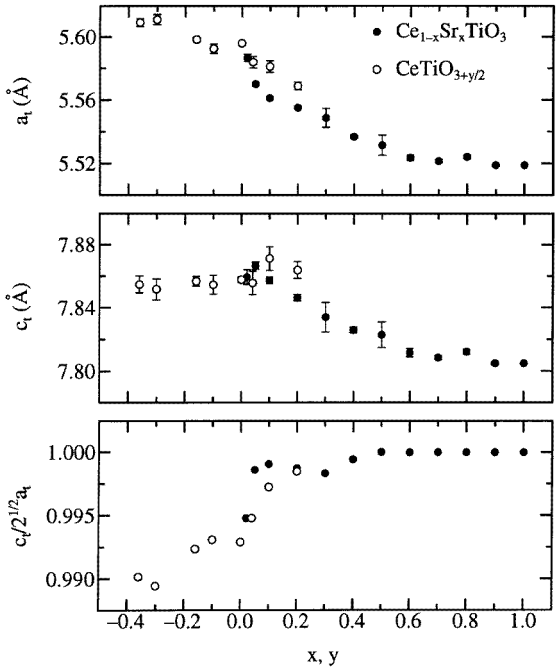

Figure 1. x and y dependences of the lattice constants and the lattice-constant ratio for $Ce_{1-x}Sr_xTiO_3$ and $CeTiO_{3+y/2}$.

constants is significant in the x and y region between 0 and 0.5; outside this the change is relatively small. Thus, the x and y dependences are not in accordance with a simple Vegard rule.

The lattice constant ratio r defined as $r = c_t/\sqrt{2}a_t$ is plotted against x and y at the bottom of figure 1. It varies significantly in the x and y region between -0.2 and 0.1. For $y \leqslant -0.2$, $r \simeq 0.990$ but, for $x,\ y \geqslant 0.1$, $r \simeq 1.000$. This suggests that a d electron for $x,\ y \leqslant 0.1$ occupies the d_{xy} orbital due to the Jahn–Teller distortion [14], while that for x, $y > 0.1$ occupies the degenerate orbitals.

3.2. Transport properties

3.2.1. Electrical resistivity. The temperature dependence of electrical resistivity ρ of $Ce_{1-x}Sr_xTiO_3$ is shown in figure 2(a) and that of $CeTiO_{3+y/2}$ is in figure 2(b). The temperature derivative of ρ in $Ce_{1-x}Sr_xTiO_3$ with $0 < x \leqslant 0.4$ is plotted in figure 2(c), where only the positive values are provided.

The resistivity data of $Ce_{1-x}Sr_xTiO_3$ may be classified into the following groups.

(i) $x = 0$. As previously reported [13], $CeTiO_3$ is a semiconductor at high temperatures, but the conduction at low temperatures may be by extended states.

(ii) $0.01 \leqslant x \leqslant 0.03$. The resistivity around room temperature is approximately proportional to temperature and its temperature derivative becomes negative around 100 K. However, the data for $x = 0.02$ appear to indicate a T^2 dependence between 150 and 250 K.

(iii) $0.04 \leqslant x \leqslant 0.4$. The resistivity above certain temperatures is expressed approximately as $\rho = \rho_0 + AT^2$, where ρ_0 is a residual resistivity and A is a constant.

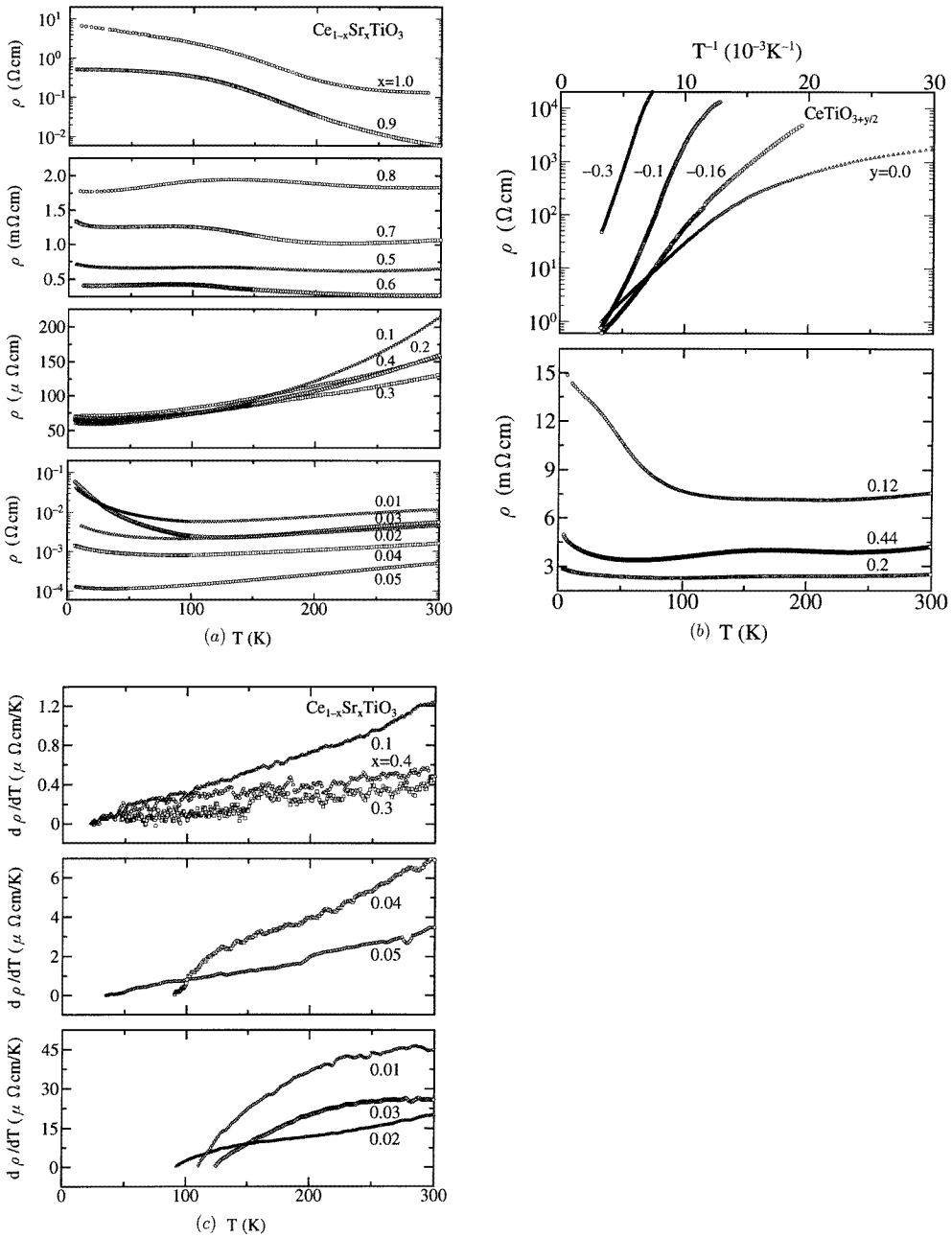

Figure 2. Temperature dependences of the electrical resistivity ρ of (a) $Ce_{1-x}Sr_xTiO_3$ and (b) $CeTiO_{3+y/2}$. The top plot is $\log\rho$ versus T^{-1}. (c) Temperature dependence of the temperature derivative of the electrical resistivity of $Ce_{1-x}Sr_xTiO_3$ with $0.01 \leqslant x \leqslant 0.4$.

The x dependence of A is shown at the top of figure 3. As shown by the full circles and dotted curve in figure 4, the temperature at which $d\rho/dT$ becomes negative decreases rapidly with increasing x for $x \leqslant 0.1$ while, for $x > 0.1$, it does not depend on x. The open

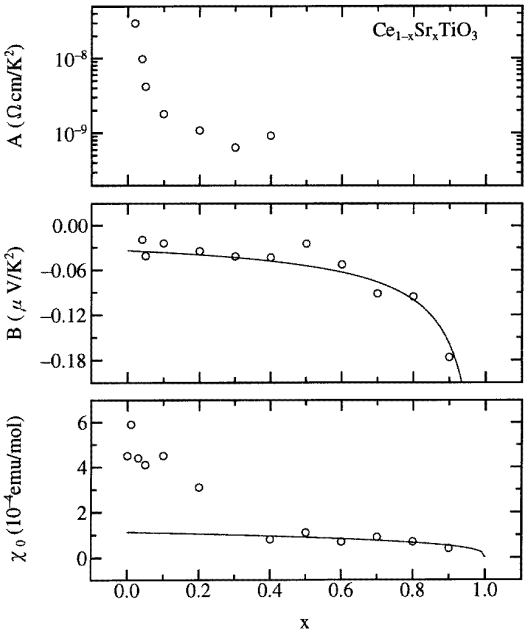

Figure 3. x dependences of the coefficient A of the T^2-term of the electrical resistivity, the coefficient B of the linear-T term of the thermoelectric power and the constant susceptibility χ_0 of $Ce_{1-x}Sr_xTiO_3$.

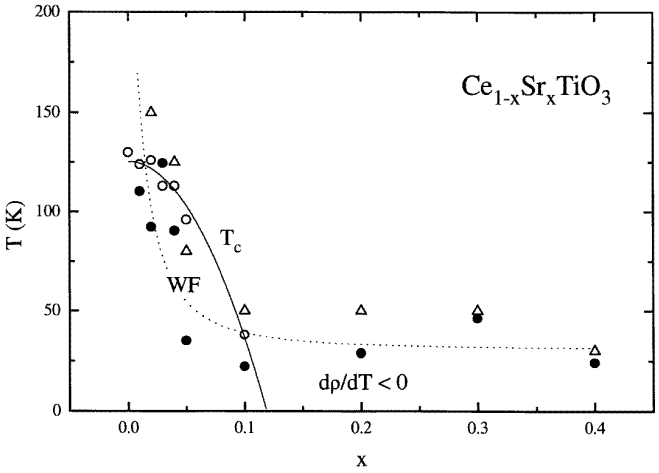

Figure 4. Phase diagram of $Ce_{1-x}Sr_xTiO_3$ with $0 \leqslant x \leqslant 0.4$: ○, magnetic transition temperatures; ●, temperatures above which $d\rho/dT$ is positive; △, temperatures above which ρ has a T^2 dependence.

triangles in figure 4 are for the temperature above which the resistivity has the T^2 term.

(iv) $0.5 \leqslant x \leqslant 0.8$. The resistivity depends little on temperature, which is reminiscent of conduction due to the impurity scattering [15].

(v) $0.9 \leqslant x \leqslant 1.0$. The resistivity is semiconductor like, but low-lying excited states

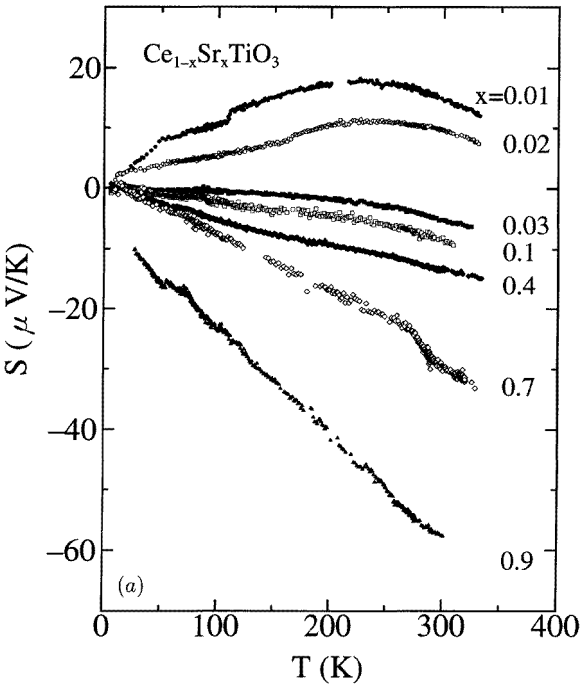

(a)

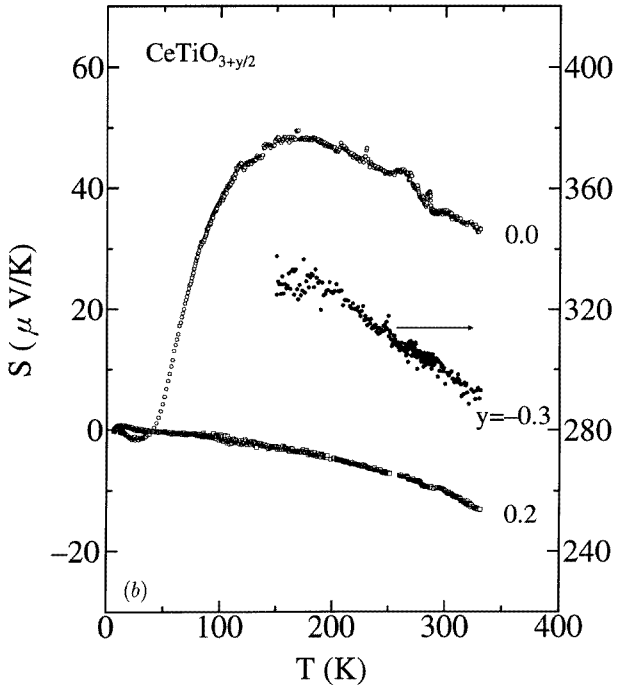

(b)

Figure 5. Temperature dependences of the thermoelectric power S of (a) $Ce_{1-x}Sr_xTiO_3$ and (b) $CeTiO_{3+y/2}$.

appear to exist.

The data for $CeTiO_{3+y/2}$ are classified as follows.

(i) The resistivity for $y < 0$ is similar to that for $CeTiO_3$ described above. However, the low-temperature behaviour where the temperature dependence of resistivity bends downwards is not pronounced for $CeTiO_{2.85}$.

(ii) The resistivity with $y = 0.12$ depends little on temperature above 100 K but, below this temperature, the resistivity increases gradually with decreasing temperature. The resistivity for $0.2 \leqslant y \leqslant 0.44$ is nearly independent of temperature, which is similar to that for $Ce_{1-x}Sr_xTiO_3$ with $0.5 \leqslant x \leqslant 0.8$.

3.2.2. Thermoelectric power. The thermoelectric power S of $Ce_{1-x}Sr_xTiO_3$ as a function of temperature is shown in figure 5(a) and that of $CeTiO_{3+y/2}$ in figure 5(b). The S data of $Ce_{1-x}Sr_xTiO_3$ with $0 \leqslant x \leqslant 0.02$ have a *positive* sign, suggesting that a major contribution to the current lies below the Fermi energy E_F. They have a round maximum and the corresponding temperature increases with increasing x. The results at low temperatures may be interpreted as characteristic of electron tunnelling between states at E_F [13, 16]. On the other hand, at high temperatures, a dominant contribution to transport comes from hopping. The data with $x \geqslant 0.03$ are *negative*, indicating electron carriers, and are approximately proportional to temperature: $S = S_0 + BT$. Here, S_0 is a constant close to zero and B is written as $-(3e)^{-1}\pi^2k^2/E_F$ where k is the Boltzmann constant, with the assumption that the conductivity is proportional to energy [17]. The x dependence of B is plotted in the middle of figure 3. The full curve in this figure is the calculated result with the effective carrier mass $m_{eff} \simeq 4m_0$, m_0 being the free-electron mass. Here, the carrier density n_{free} is assumed to be expressed as $n_{free} = 1.6 \times 10^{22}(1-x)$. The agreement between experimental and calculated results appears to be rather satisfactory.

For $CeTiO_{3+y/2}$ with $y \leqslant 0$, S is *positive* and increases with decreasing y. The relatively large value, about 3×10^2 μV K^{-1}, for $CeTiO_{2.85}$ and its temperature dependence indicate that this compound is essentially semiconducting. On the other hand, for $y = 0.2$, S is *negative*. Its temperature dependence at low temperatures is approximately linear and similar to that for $Ce_{1-x}Sr_xTiO_3$ with $x \geqslant 0.03$.

3.2.3. Hall coefficient. The Hall coefficients R_H at 290 K for $Ce_{1-x}Sr_xTiO_3$ with $x \geqslant 0.02$ and for $CeTiO_{3+y/2}$ with $y \geqslant -0.02$ show a *negative* sign. The carrier concentration n estimated from a one-band model as a function of x and y is shown in figure 6. The data for $Ce_{1-x}Sr_xTiO_3$ are compatible with those for $CeTiO_{3+y/2}$. The full line in this figure shows the carrier concentration n_{free} calculated from the free-electron relationship as defined above. For $0.2 \leqslant x, y \leqslant 0.9$, n agrees roughly with n_{free} but, for $x, y \leqslant 0.1$, n is significantly smaller than n_{free}. A reduction in n has not been reported for $La_{1-x}Sr_xTiO_3$ [7].

3.3. Magnetic properties

The inverse of the magnetic susceptibility χ for $Ce_{1-x}Sr_xTiO_3$ as a function of temperature is shown in figure 7(a) and that for $CeTiO_{3+y/2}$ in figure 7(b). This does not contain the data in the temperature region where the remanent magnetization appears significantly. All the data show a Curie–Weiss-like temperature dependence.

The magnetic susceptibility of the present system is expressed as $\chi = \chi_d + \chi_f + \chi_{orb} + \chi_{dia}$, where the subscripts d and f refer to contributions from the corresponding spins, and where the subscripts orb and dia are for contributions from Van Vleck orbital

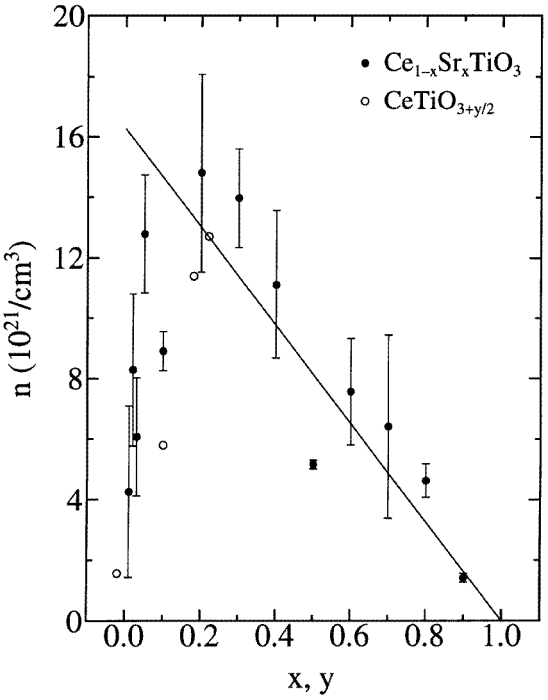

Figure 6. x and y dependences of the carrier density n of $Ce_{1-x}Sr_xTiO_3$ and $CeTiO_{3+y/2}$ estimated from the Hall coefficient.

paramagnetism and diamagnetism, respectively. Here, the last two contributions are usually temperature independent. Previously, we have shown that, below 300 K, the temperature dependence of χ_d for Ti ions in $RTiO_3$, where R = Ce, Pr or Nd, is negligibly small compared with that of χ_f [13]. Analysis of χ_f based on the Curie–Weiss law indicates that the Curie constant of 4f spins is approximately 10% smaller than that of free ions due to the crystalline electric field (CEF) effect. The evidence for Ce^{3+} has also been obtained by x-ray absorption spectroscopy [18].

With the assumption of tetragonal symmetry around Ce^{3+}, the CEF Hamiltonian of the ground-state multiplet of $^2F_{5/2}$ is $H_{CEF} = B_2^0O_2^0 + B_4^0O_4^0 + B_4^4O_4^4$, where B_n^m are the CEF parameters and O_n^m are the corresponding Stevens operators [19]. The magnitudes for the CEF level of Ce^{3+} in $CeTiO_3$ are estimated to be $B_2^0 = -5.1$ K, $B_4^0 = -2.2$ K, and $B_4^4 = 21$ K from the full curve in figure 7(b), which are close to the values for Ce^{3+} in $CeVO_3$ [11]. The temperature-independent susceptibility χ_0 defined as $\chi_0 = \chi_d + \chi_{orb} + \chi_{dia}$ is about 4.5×10^{-4} emu mol^{-1}. For simplicity, the following discussion assumes that the CEF parameters do not depend on chemical composition or crystal symmetry since, in order to estimate them precisely, we have to know the temperature dependence of χ_d at high temperatures. Therefore, χ_f is taken to depend on only the Ce concentration. The full curves in figure 7(a) provide the x dependence of χ_0 as shown at the bottom of figure 3, where the Ce concentrations estimated by this analysis agree with those of the nominal chemical formula with an accuracy of 10%. Below $x = 0.3$, χ_0 is suggested to increase significantly as x decreases. The full curve at the bottom of figure 3 that is based on a free-electron relationship with $m_{eff} \simeq 5m_0$ correlates with the results for $x \geqslant 0.4$ when it

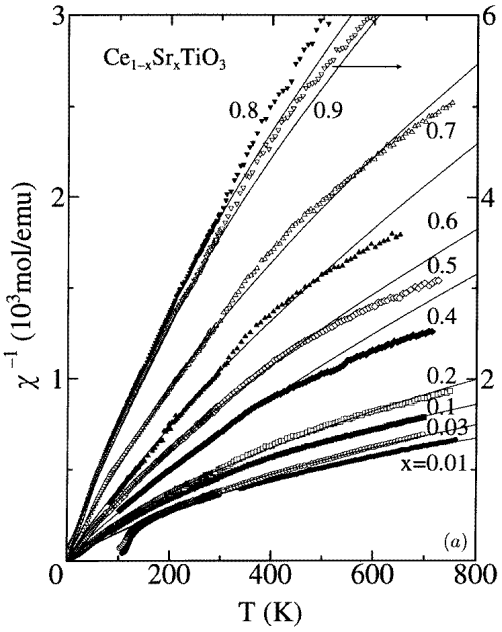

(a)

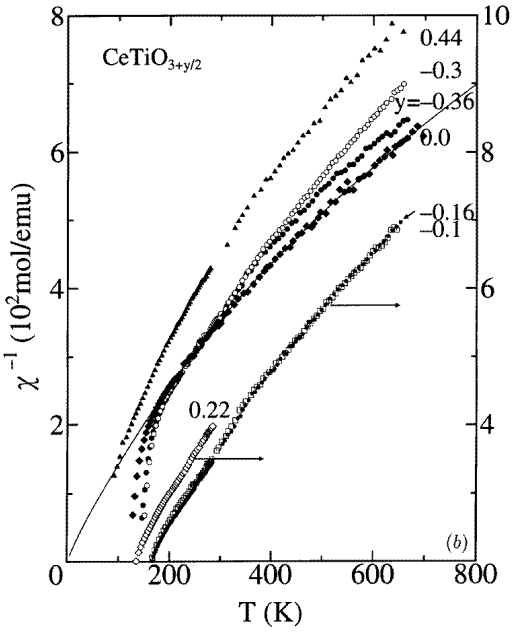

(b)

Figure 7. Temperature dependences of the inverse magnetic susceptibility χ^{-1} of (a) $Ce_{1-x}Sr_xTiO_3$ and (b) $CeTiO_{3+y/2}$, where the full curves are the calculated results.

is assumed that $\chi_{orb} + \chi_{dia} = 0$ and the Wilson ratio is unity.

At low temperatures, the remanent magnetization σ defined as $M = \chi H + \sigma$ appears for $Ce_{1-x}Sr_xTiO_3$ with $x \leqslant 0.1$ in the measured region above 4.2 K and for $CeTiO_{3+y/2}$ with $y \leqslant 0.22$ above 80 K. This is qualitatively understood in terms of the molecular field of the canted moment of Ti ions acting on the 4f spins of Ce ions [13]. The temperature T_c below which σ appears for $Ce_{1-x}Sr_xTiO_3$ is shown in figure 4 by the open circles and the full curve.

4. Discussion

4.1. Electronic states of $Ce_{1-x}Sr_xTiO_3$ and $CeTiO_{3+y/2}$ with x, $y > 0.1$

In the region of $x > 0.1$ for $Ce_{1-x}Sr_xTiO_3$, measurements of the Hall coefficient provide the total number of carriers expected from the chemical formula. Both the Hall coefficient and the thermoelectric power indicate that the carriers are electrons. The crystal changes from pseudotetragonal to cubic at $x = 0.5$ with increasing x. Above this concentration except for $x \simeq 1$, the resistivity is nearly temperature independent. This may indicate that the electron transport is correlated partly with the crystal symmetry. Since the nearly cubic phase has approximately 180° linkage for the Ti-O–Ti path, the band width is expected to be larger than that of the pseudotetragonal phase. We should note that the resistivity of cubic $SrVO_3$ with d^1 has a T^2 dependence [12]. Therefore, a negligible contribution of the T^2 term may be attributed to the decreases in U/W and the carrier concentration. Moreover, a large contribution probably from the impurity scattering for $x \geqslant 0.5$ suggests that the random potential from the $Ce_{1-x}Sr_x$ ions is responsible for the transport mechanism. Based on the present data, the mean free path of carriers in that x region is found to be actually comparable with the Ti–Ti distance. As shown in figure 3, the coefficient B of the linear-T term of the thermoelectric power for $0.1 < x \leqslant 0.9$ and the constant susceptibility χ_0 for $x \geqslant 0.4$ follow a free-electron model with $m_{eff} \simeq 4m_0$ and $m_{eff} \simeq 5m_0$, respectively. Here, the slight difference between m_{eff}-values for $x \geqslant 0.4$ may be due to an underestimation of the orbital susceptibility and/or the Wilson ratio. Therefore, the electronic states for $0.4 \leqslant x \leqslant 0.9$ are free electron like with an enhancement of m_{eff}, and the transport mechanism is changed significantly between $x = 0.4$ and 0.5.

On the other hand, for $0.1 < x < 0.4$, χ_0 increases with decreasing x. This is consistent with the result that the conduction electron mass in the metallic phase increases drastically with a constant Wilson ratio [7]. However, the coefficient A of the T^2-term of the resistivity, which is expected to be proportional to m_{eff}^2 in the Fermi liquid [20], and B do not show a significant enhancement of m_{eff}. In order to clarify this point, further investigations are necessary. In particular, we have to obtain a precise expression of the thermoelectric power based on the actual band structure. The resistivity minimum at low temperatures for $0.1 < x \leqslant 0.4$, where the mean free path of carriers is appreciably larger than the Ti–Ti distance, may be due to a localization effect by a random potential.

The above discussion may be applied to $CeTiO_{3+y/2}$, because the results of lattice constant, thermoelectric power and Hall coefficient are comparable with those of $Ce_{1-x}Sr_xTiO_3$. Here, we should note that $CeTiO_{3+y/2}$ has a significant cation vacancy or lattice imperfection. This will provide a larger random potential effect than the Ce–Sr substitution. While the resistivity does not show a T^2 dependence for the expected concentration, it may be characterized as conduction by impurity scattering.

4.2. Electronic states of $Ce_{1-x}Sr_xTiO_3$ and $CeTiO_{3+y/2}$ with x, $y \leqslant 0.1$

In the region of x, $y \leqslant 0.1$, the total number of carriers estimated from measurements of the Hall coefficient is smaller than the expected value from the chemical formula. For $x \geqslant 0.03$ and $y \geqslant -0.02$, both the Hall coefficient and the thermoelectric power indicate that the carriers are electrons. However, for $x \leqslant 0.02$, the Hall coefficient and the thermoelectric power indicate opposite signs, i.e. electron and hole carriers, respectively. This is probably due to an anomaly of band dispersion. Another possibility would be transport by polaron-like hopping based on a model described by Friedman and Holstein [21].

As shown in figure 3, A increases rapidly with decreasing x and has a maximum around $x = 0.02$. However, for $x = 0.01$ and 0.03, the T^2 term is negligible. This is probably due to an inhomogeneous distribution of atoms. For $x \leqslant 0.01$, the contribution of the T^2 term of the resistivity is negligible and a variable-range hopping-like state appears. For the thermoelectric power, the apparent agreement between experimental and calculated results may be accidental. In this x region, we may have to consider a band structure with a pseudogap [13] or a dispersion anomaly, and thus our applied model to the thermoelectric power is oversimplified. χ_0 is significantly larger than the calculated value from a free-electron relationship with $m_{eff} \simeq 5m_0$. These results are partly correlated with an increase in U/W due to the significant Jahn–Teller effect.

It should be noted that, for $x \leqslant 0.1$, the remanent magnetization based on an antisymmetric interaction of Ti ions appears and the transition temperature T_c increases with decreasing x as shown in figure 4. T_c does not always correspond to the temperature at which the sign of $\mathrm{d}\rho/\mathrm{d}T$ changes, but the temperature below which the T^2 term of the resistivity is negligible. Therefore, the rapid increase in A with decreasing x may be attributed to an enhancement of the carrier mass [22] as well as to an antiferromagnetic correlation effect. For $x > 0.1$, the remanent magnetization does not appear, probably owing to the larger band width and/or weaker strength of antiferromagnetic instability. This does not lead to an increase in A through an antiferromagnetic correlation. The present result is apparently consistent with the spin fluctuation theory for heavy-electron systems [23].

5. Conclusion

We have studied the electronic states of the perovskite-type $Ce_{1-x}Sr_xTiO_3$ ($0 \leqslant x \leqslant 1$) and $CeTiO_{3+y/2}$ ($-0.36 \leqslant y \leqslant 0.44$) systems with a metal–insulator transition through measurements of x-ray diffraction, electrical resistivity, thermoelectric power, Hall effect and magnetization. The $Ce_{1-x}Sr_xTiO_3$ system is pseudotetragonal for $x \leqslant 0.4$ and cubic for $x \geqslant 0.5$. The properties are as follows: for $0 \leqslant x < 0.02$, variable-range hopping-like insulators; for $0.04 \leqslant x \leqslant 0.4$, highly correlated metals accompanied by a significant Jahn–Teller effect, a band dispersion anomaly and cant magnetism for $x \leqslant 0.1$; for $0.5 \leqslant x \leqslant 0.9$, metals with a mean free path comparable with the Ti–Ti distance; for $x = 1$, band insulators. The properties of $CeTiO_{3+y/2}$ and $Ce_{1-x}Sr_xTiO_3$ are closely comparable, but larger random potentials due to the atomic deficiencies in the former system make the electronic states there more complicated. A broad-band semiconductor-like conduction appears only for $CeTiO_{2.85}$. For the metallic state towards the boundary between the Mott–Hubbard insulator and metal, it may be necessary to consider both an enhancement of the conduction electron mass and the antiferromagnetic correlation effect. Spin fluctuation effects in the present systems should be examined by another experiment.

The critical concentration for the transition between the band insulator $SrTiO_3$ and metals is unclear. This may mean that the wavefunction of electron carriers extends to the

neighbouring Ti–Ti distance even for a low Ce concentration. The critical probability of the simple-cubic lattice for the connectivity of the electrons is expected to be smaller than the percolation threshold [24]. It may be interesting to study the site preference for carriers in such a metal–insulator transition as has been tested in the vanadium spinels [25].

Previous investigations of $La_{1-x}Sr_xTiO_3$ and $Y_{1-x}Ca_xTiO_3$ without 4f electrons have emphasized only an enhancement of the conduction electron mass in the vicinity of the transition between the Mott insulator and the correlated metal. We consider that the various characteristics revealed in this work may be general properties for the perovskite-type Ti oxide system with cant magnetism in certain regions of the carrier concentration and the band width. In fact, we have confirmed similar properties for $La_{1-x}Sr_xTiO_3$ to those described here [26].

Acknowledgments

We thank Professor D S Hirashima and Professor A Fujimori for valuable discussions.

References

[1] Mott N F 1990 *Metal–Insulator Transitions* 2nd edn (London: Taylor & Francis)
[2] For a review, Georges A, Kotliar G, Krauth W and Rozenberg M J 1996 *Rev. Mod. Phys.* **68** 13
[3] Greedan J E 1985 *J. Less-Common Met.* **111** 335 and references therein
[4] Lichtenberg F, Widmer D, Bednorz J G, Williams T and Reller A 1991 *Z. Phys.* B **82** 211
[5] Sunstrom J E IV, Kauzlarich S M and Klavins P 1992 *Chem. Mater.* **4** 346
[6] Crandles D A, Timusk T, Garrett J D and Greedan J E 1992 *Physica* C **201** 407
[7] Katsufuji T and Tokura Y 1994 *Phys. Rev.* B **50** 2704 and references therein
[8] Ju H L, Eylem C, Peng J L, Eichhorn B W and Greene R L 1994 *Phys. Rev.* B **49** 13 335
[9] Nguyen H C and Goodenough J B 1995 *Phys. Rev.* B **52** 8776
[10] Morikawa K, Mizokawa T, Fujimori A, Taguchi Y and Tokura Y 1996 *Phys. Rev.* B **54** 8446 and references therein
[11] Onoda M and Nagasawa H 1996 *Solid State Commun.* **99** 487
[12] Onoda M, Ohta H and Nagasawa H 1991 *Solid State Commun.* **79** 281
[13] Onoda M and Yasumoto M 1997 *J. Phys.: Condens. Matter* **9** 3861
[14] Goodenough J B 1971 *Prog. Solid State Chem.* **5** 145
[15] Ziman J M 1979 *Electrons and Phonons* (Oxford: Oxford University Press)
[16] Brenig W, Döhler G H and Wölfle P 1973 *Z. Phys.* **258** 381
[17] Wilson A H 1958 *The Theory of Metals* 2nd edn (London: Cambridge University Press)
[18] Akaki O, Chainani A, Yokoya T, Fujisawa H, Takahashi T and Onoda M 1997 preprint
[19] Abragam A and Bleaney B 1970 *Electron Paramagnetic Resonance of Transition Ions* (Oxford: Oxford University Press)
[20] Kadowaki K and Woods S B 1986 *Solid State Commun.* **58** 507
[21] Friedman L and Holstein T 1963 *Ann. Phys.* **21** 474
[22] Brinkman W F and Rice T M 1970 *Phys. Rev.* B **2** 4302
[23] Takimoto T and Moriya T 1996 *Solid State Commun.* **99** 457
[24] Essam J W 1972 *Phase Transitions and Critical Phenomena* vol 2, ed C Domb and M S Green (London: Academic) p 197
[25] Onoda M, Imai H, Amako Y and Nagasawa H 1997 *Phys. Rev.* B at press
[26] Onoda M and Kohno M 1997 unpublished